Tropical wetland characterization with Polarimetric SAR

Shimon Wdowinski[(1)] and Sang-Hoon Hong [(1)(2)]

(1) University of Miami, U.S.A.
(2)Korea Aerospace Research Institute, Korea

Contribution to the ESA's supported project
POLSAR-AP

Presentation content

- Tropical wetlands
- Characterization of Tropical wetlands
- Characterization using Polarimetric SAR observations – Decompositions
- Study area – the Everglades
- Everglades Decompositions
- Conclusions
- Acknowledgments

Tropical wetland forests

Ecosystem that are inundated or saturated all year or part of the year. Wet conditions drive ecosystem processes and functions, supporting unique biological communities physically and physiologically adapted to a wet (hydric) environment.

Mangroves

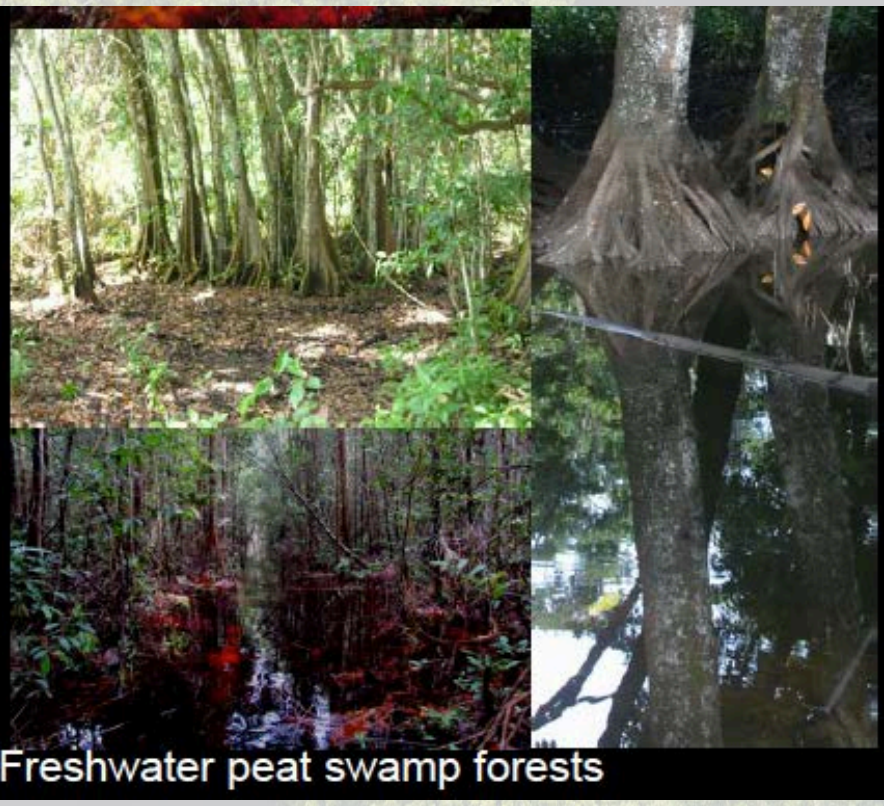

Freshwater peat swamp forests

Ecosystem Services

The processes by which the environment produces resources that we often take for granted such as:

- clean water,
- timber,
- habitat for fisheries, and
- pollination of native and agricultural plants.

Biological Diversity

Many flagship species for conservation find refuge in wetland forests. Countless plants, fungi, fish and insects remain poorly known or undescribed

Threats to Tropical Wetland Forests

- Anthropogenic:

  Logging, land conversion, drainage, fire, invasive species

- Natural:

  Sea level rise, climate change (more extreme events)

Wetland characterization

- Land cover classification
- Monitoring land cover changes
- Typically based on optical remote sensing imagery (problematic in the tropics)

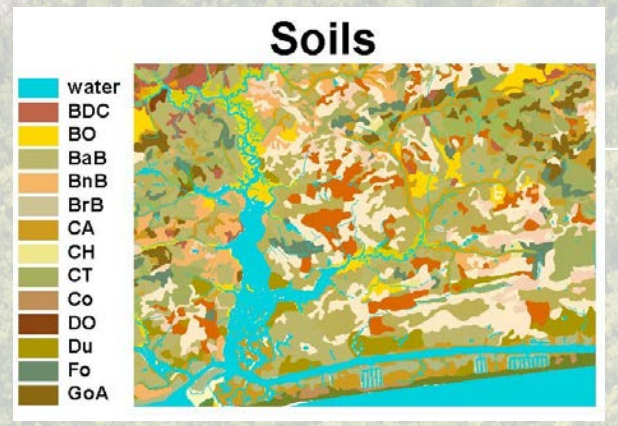

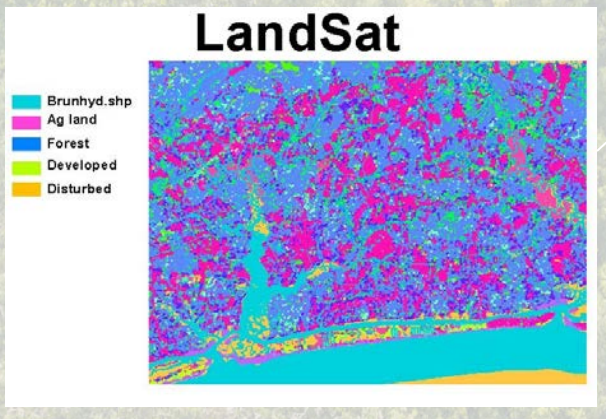

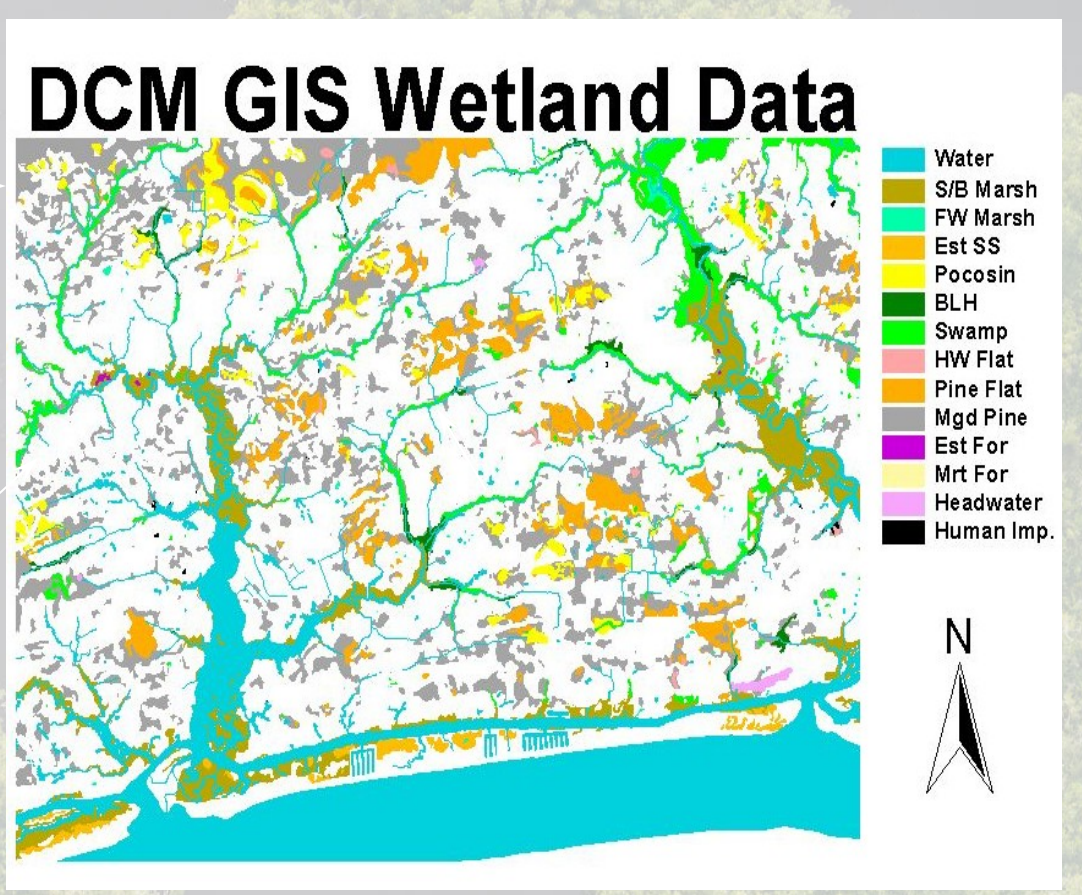

Pol-SAR Wetland characterization

- Land cover classification
- Monitoring land cover changes
- Works at all weather conditions

S_{hh} S_{vv} S_{hv}

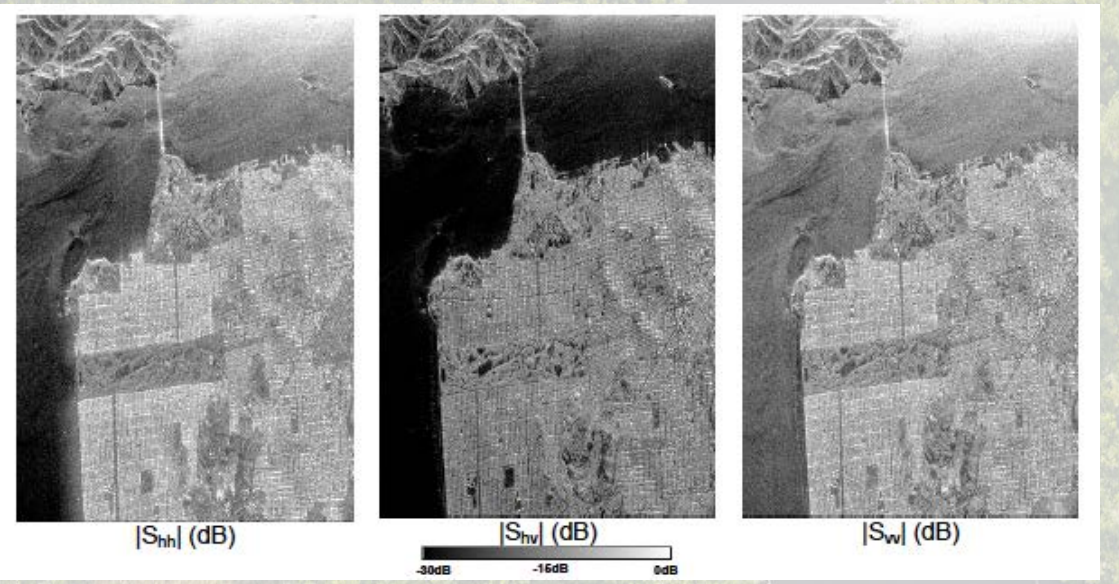

Pauli decomposition

Lopez-Martinez et al. (2005)

Freeman Decomposition

$$\boldsymbol{T} = P_s \boldsymbol{T}_{\text{surface}} + P_d \boldsymbol{T}_{\text{double}} + P_v \boldsymbol{T}_{\text{volume}}$$

Ps Pd Pv

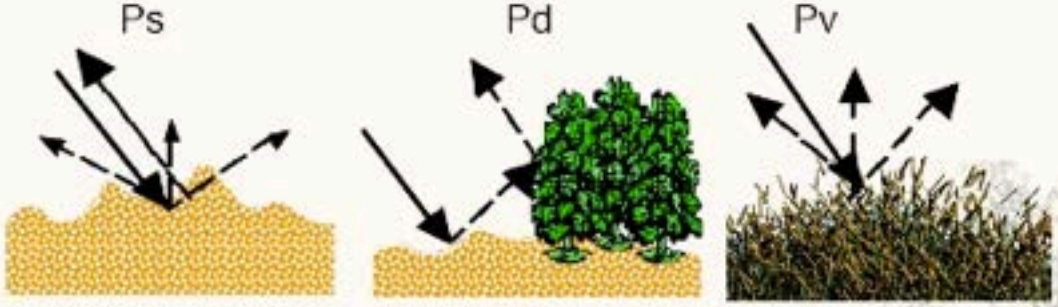

$$T = \begin{bmatrix} T_{11} & T_{12} & 0 \\ T_{12}^* & T_{22} & 0 \\ 0 & 0 & T_{33} \end{bmatrix}$$

$$= f_s \begin{bmatrix} 1 & \beta^* & 0 \\ \beta & |\beta|^2 & 0 \\ 0 & 0 & 0 \end{bmatrix} + f_d \begin{bmatrix} |\alpha|^2 & \alpha & 0 \\ \alpha^* & 1 & 0 \\ 0 & 0 & 0 \end{bmatrix} + \frac{f_v}{4} \begin{bmatrix} 2 & 0 & 0 \\ 0 & 1 & 0 \\ 0 & 0 & 1 \end{bmatrix}$$

Jiao et al. (2011)

Yamaguchi Decomposition

Four-component Scattering Power Decomposition

$$\langle [T] \rangle = f_s \langle [T] \rangle_{surface} + f_d \langle [T] \rangle_{double} + f_v \langle [T] \rangle_{vol} + f_c \langle [T] \rangle_{helix}$$

Measured = Surface scattering + Double bounce + Volume scattering + Helix scattering

expansion matrix

$$\begin{bmatrix} 1 & \beta^* & 0 \\ \beta & |\beta|^2 & 0 \\ 0 & 0 & 0 \end{bmatrix} \qquad \begin{bmatrix} |\alpha|^2 & \alpha & 0 \\ \alpha^* & 1 & 0 \\ 0 & 0 & 0 \end{bmatrix}$$

$$\frac{1}{30}\begin{bmatrix} 15 & 5 & 0 \\ 5 & 7 & 0 \\ 0 & 0 & 8 \end{bmatrix} \quad \frac{1}{4}\begin{bmatrix} 2 & 0 & 0 \\ 0 & 1 & 0 \\ 0 & 0 & 1 \end{bmatrix} \quad \frac{1}{30}\begin{bmatrix} 15 & -5 & 0 \\ -5 & 7 & 0 \\ 0 & 0 & 8 \end{bmatrix}$$

$$\frac{1}{2}\begin{bmatrix} 0 & 0 & 0 \\ 0 & 1 & \pm j \\ 0 & \mp j & 1 \end{bmatrix}$$

Scattering Power

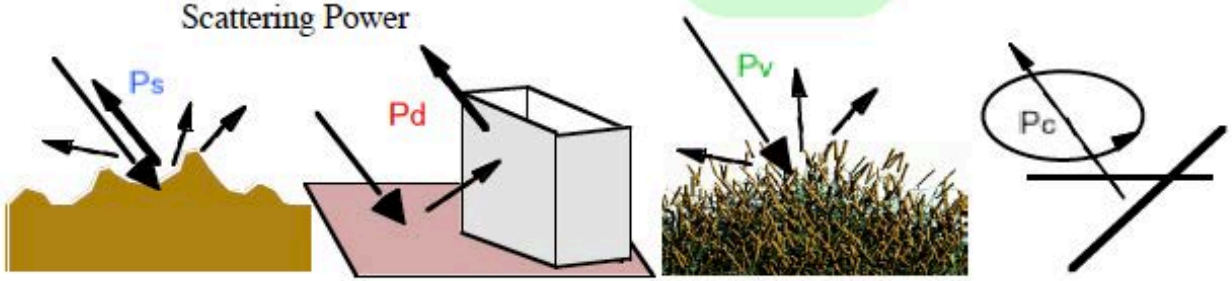

Yajima et al. (2008)

Hong & Wdowinski Decomposition –

Four component scattering with cross-pol double bounce

$$\langle [T] \rangle = f_s \langle [T] \rangle_{surface} + f_d \langle [T] \rangle_{double} + f_{rd} \langle [T] \rangle_{\substack{rotated \\ dihedral}} + f_v \langle [T] \rangle_{vol}$$

Measured = Surface scattering + Co-Pol Dounbel bounce + Cross-Pol Double bounce + Volume scattering

Scattering Power

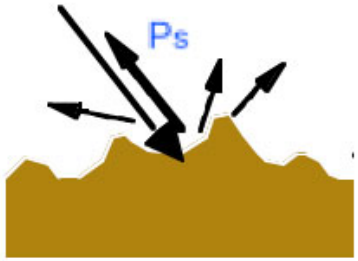

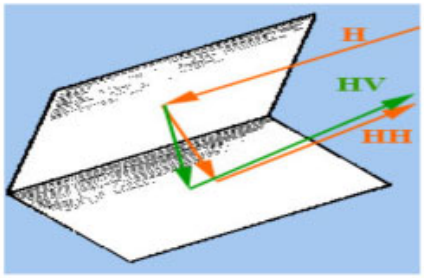

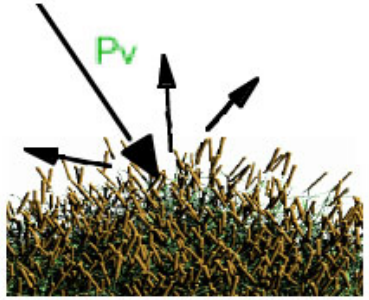

Hong & Wdowinski (2013)

Cross-pol scattering [S_{hv}]

- Most decompositions assume that the cross-pol component (Shv) represents solely volume scattering, which implies unstable scatters in vegetated areas.
- However, we found coherent cross-pol interferograms in vegetated wetland environment, indicating that some cross-pol scatters are very stable.
- Furthermore, the similar fringe patterns in co- and cross-pol interefrograms suggest that some of the cross-pol signal samples the aquatic surface beneath the vegetation.

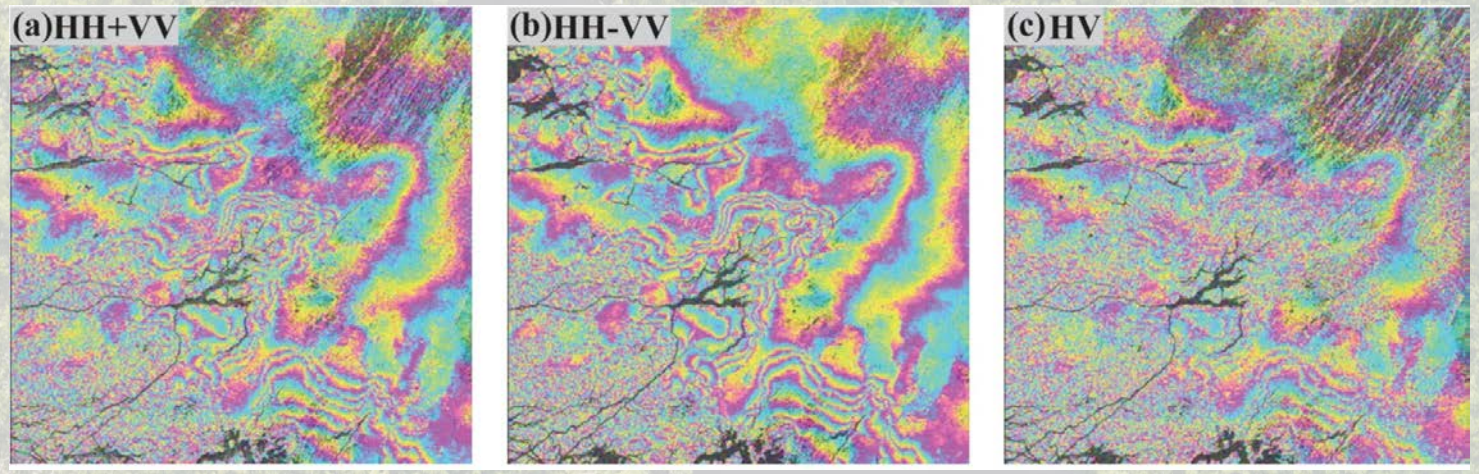

Dihedral and rotated dihedral

Dihedral

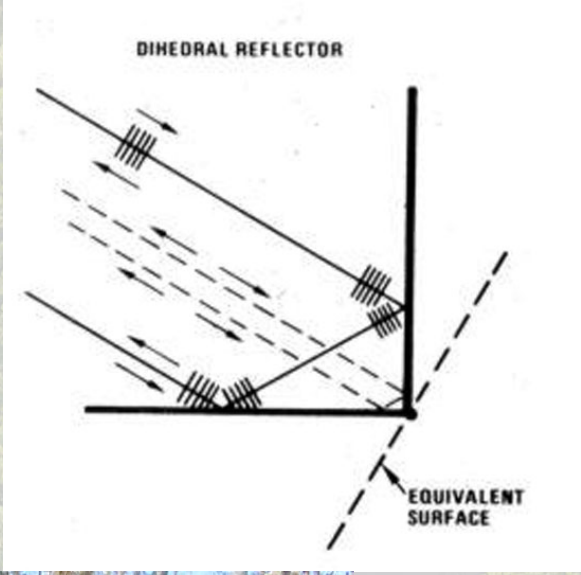

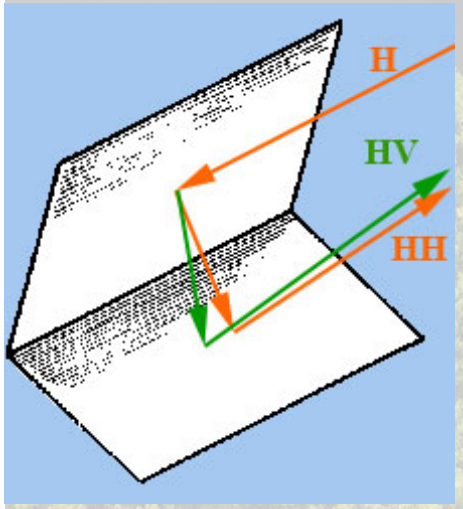

Rotated Dihedral

Cypress

Mangroves

Four component Scattering Target Decomposition

$$\langle [T] \rangle = f_s \langle [T] \rangle_{surface} + f_d \langle [T] \rangle_{double} + f_{rd} \langle [T] \rangle_{\substack{rotated \\ dihedral}} + f_v \langle [T] \rangle_{vol}$$

Measured = Surface scattering + Co-Pol Dounbel bounce + Cross-Pol Double bounce + Volume scattering

Scattering Power

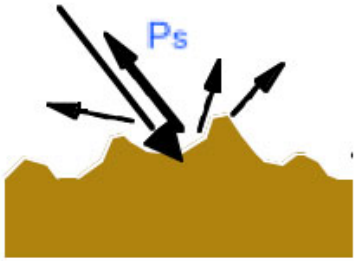

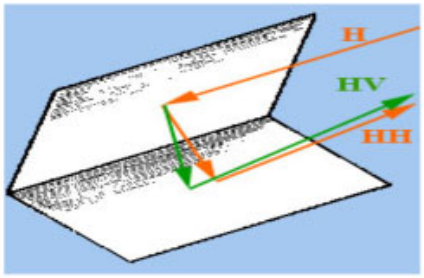

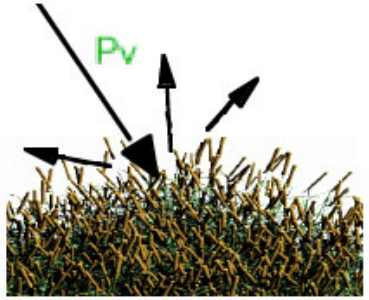

Hong & Wdowinski (H-W) Decomposition (2013)

Study area – The Everglades

- Unique wetland environment
- The only tropical wetlands in the US
- Contains both coastal and inland wetlands

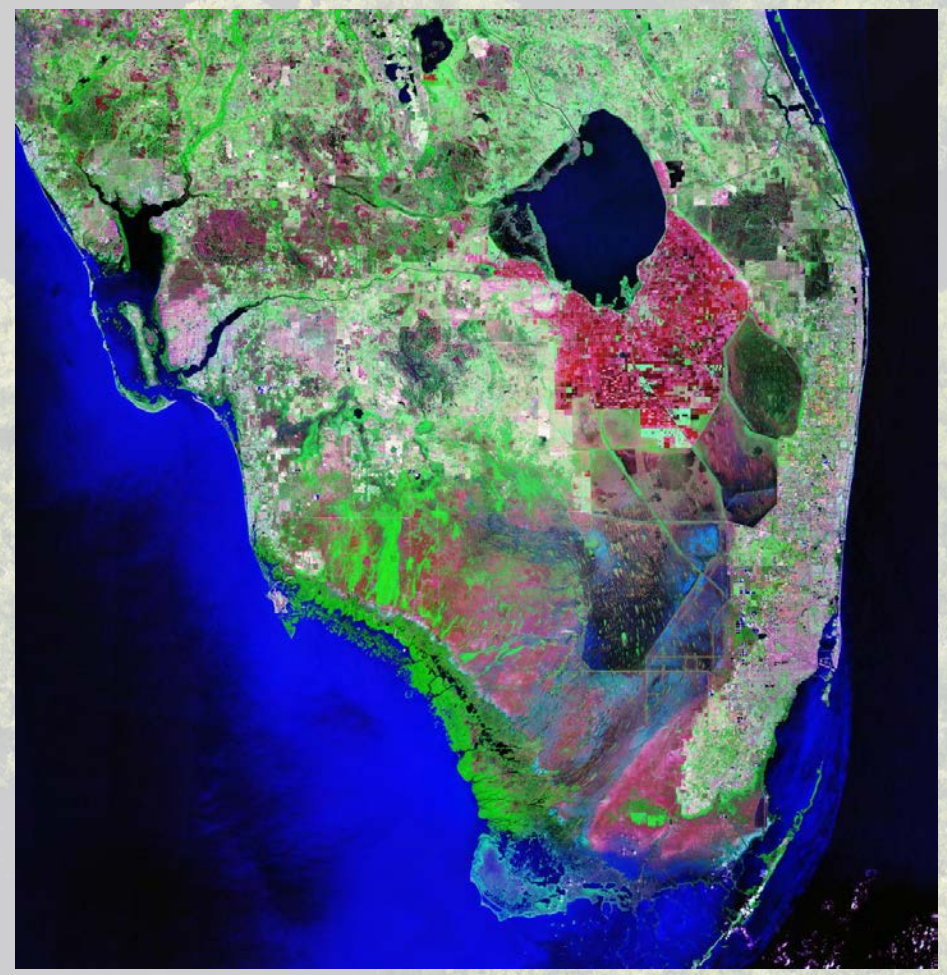

Pol-SAR data

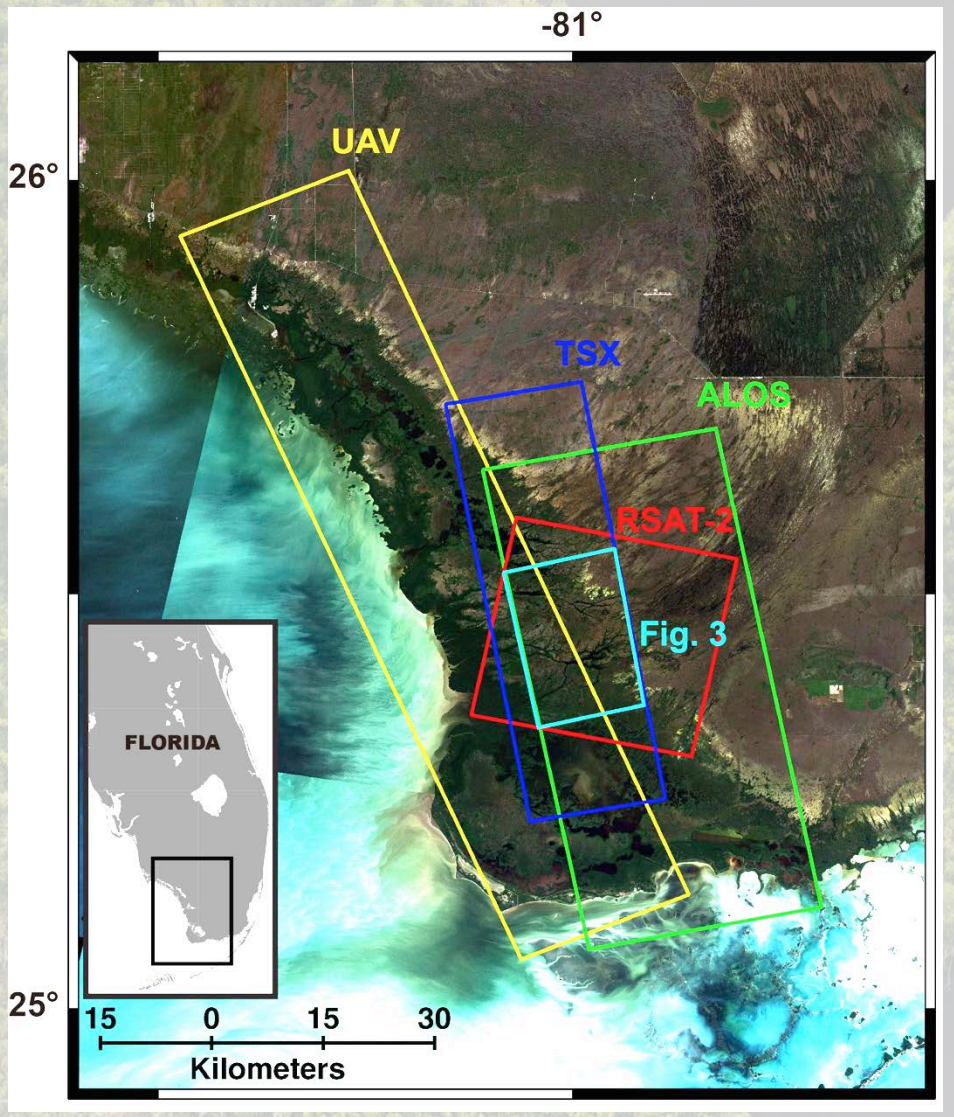

Sensor	Freq.	Resolution Az. X Rng (m)
TSX	X-band (3.1 cm)	2.40 x 0.91
RSAT-2	C-band (5.6 cm)	4.70 x 4.73
ALOS	L-band (24.1 cm)	3.56 x 9.37
UAVSAR	L-band (24.1 cm)	7.20 x 5.00

Decompositions – Radarsat-2

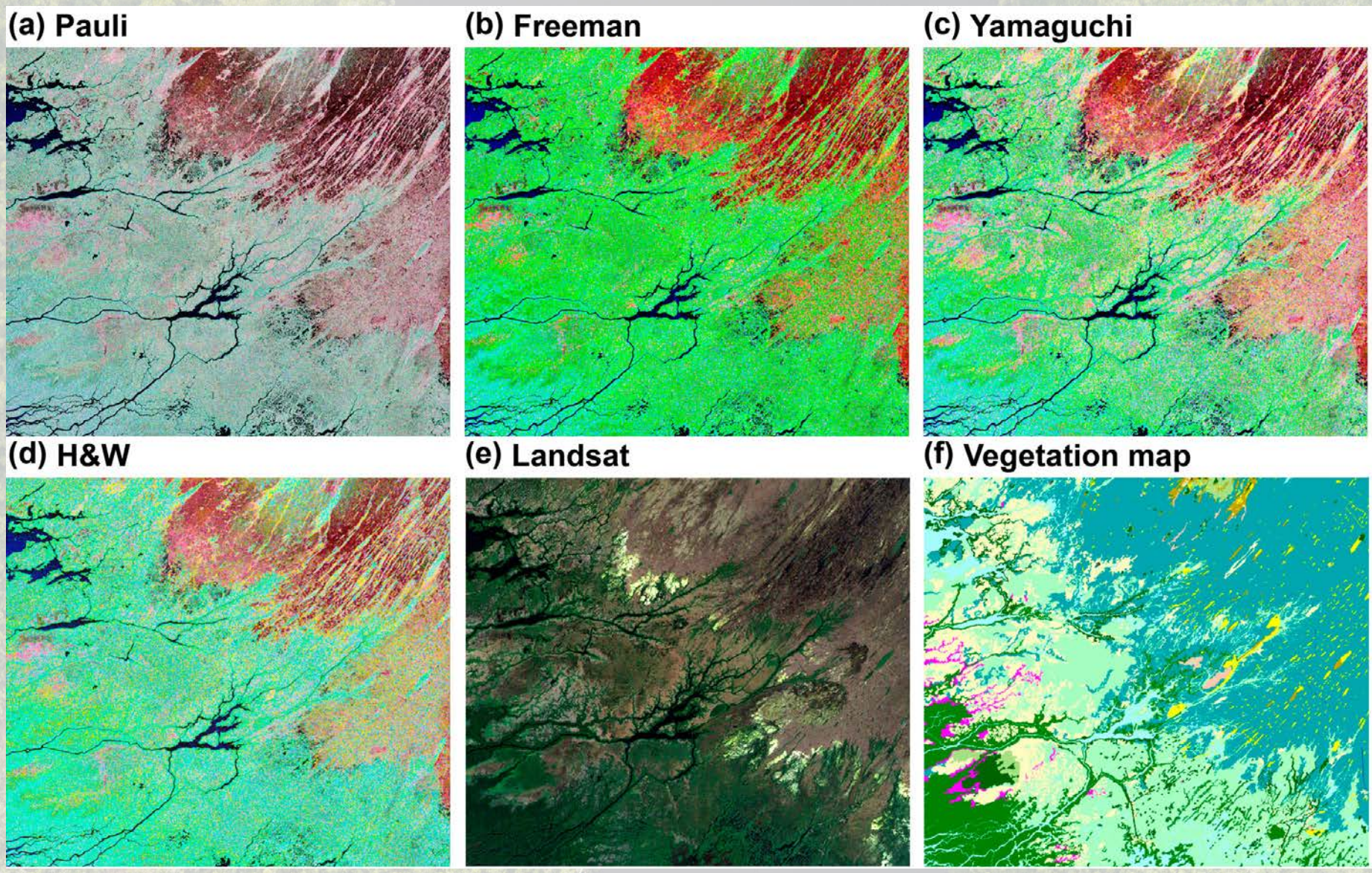

X-, C-, and L- band Decompositions

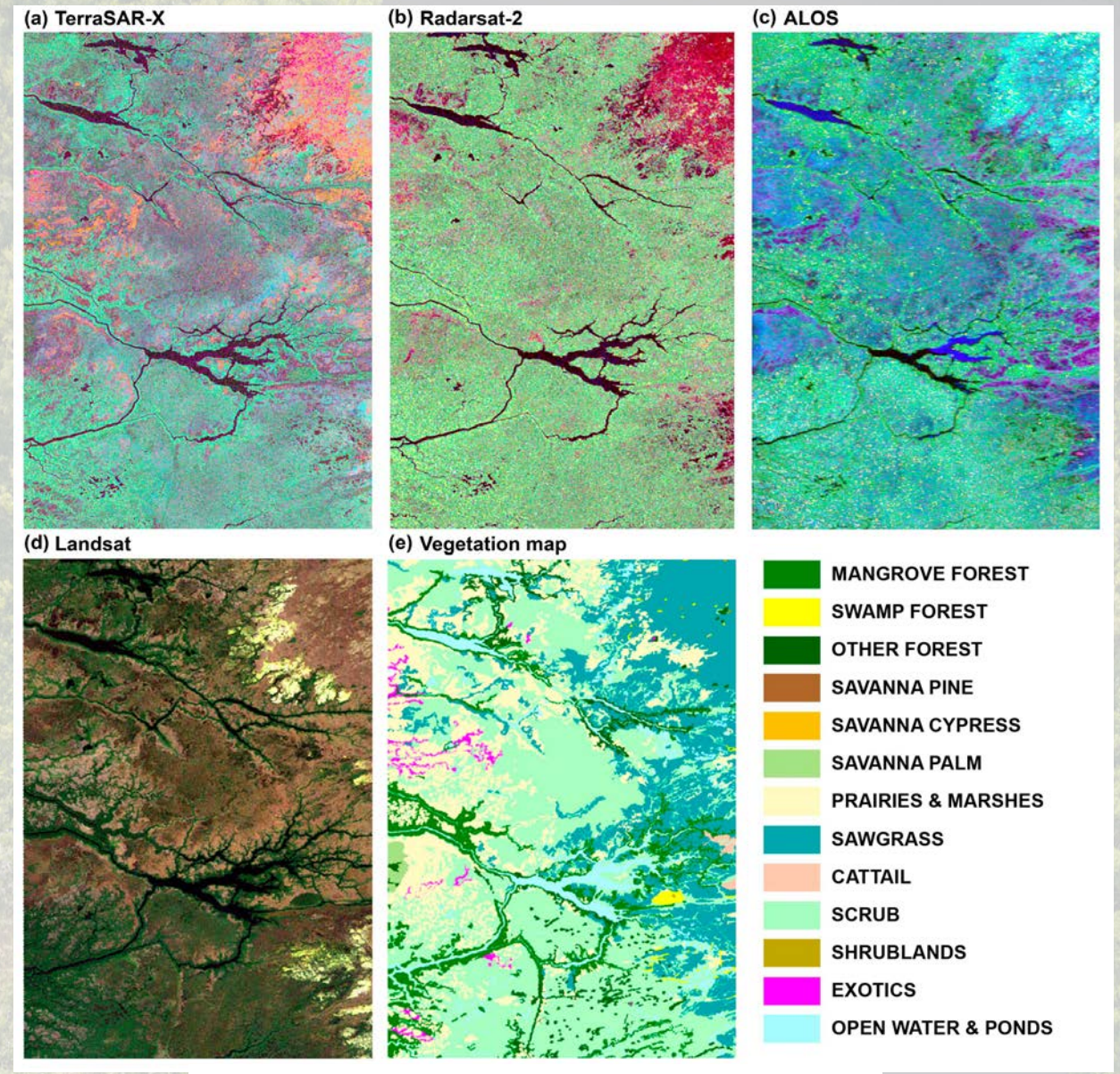

Decomposed image (Ps, Pd, Pv)

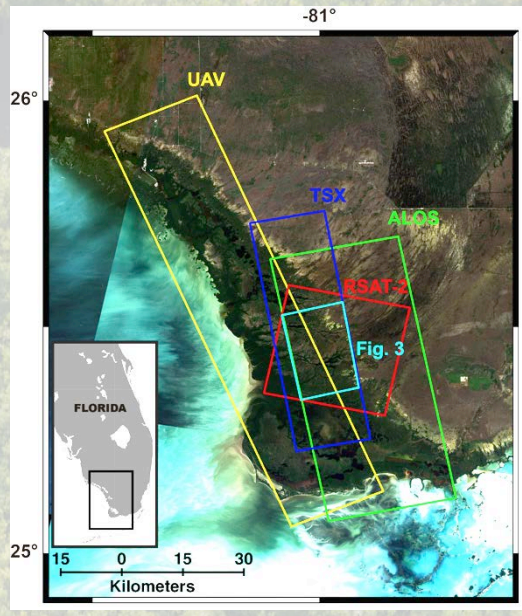

Freshwater scattering

X- & C-band – Double

L-band - Surface

Sensitivity

X- & L-bands – High

C-band - Low

H&W Decomposition

Classifications

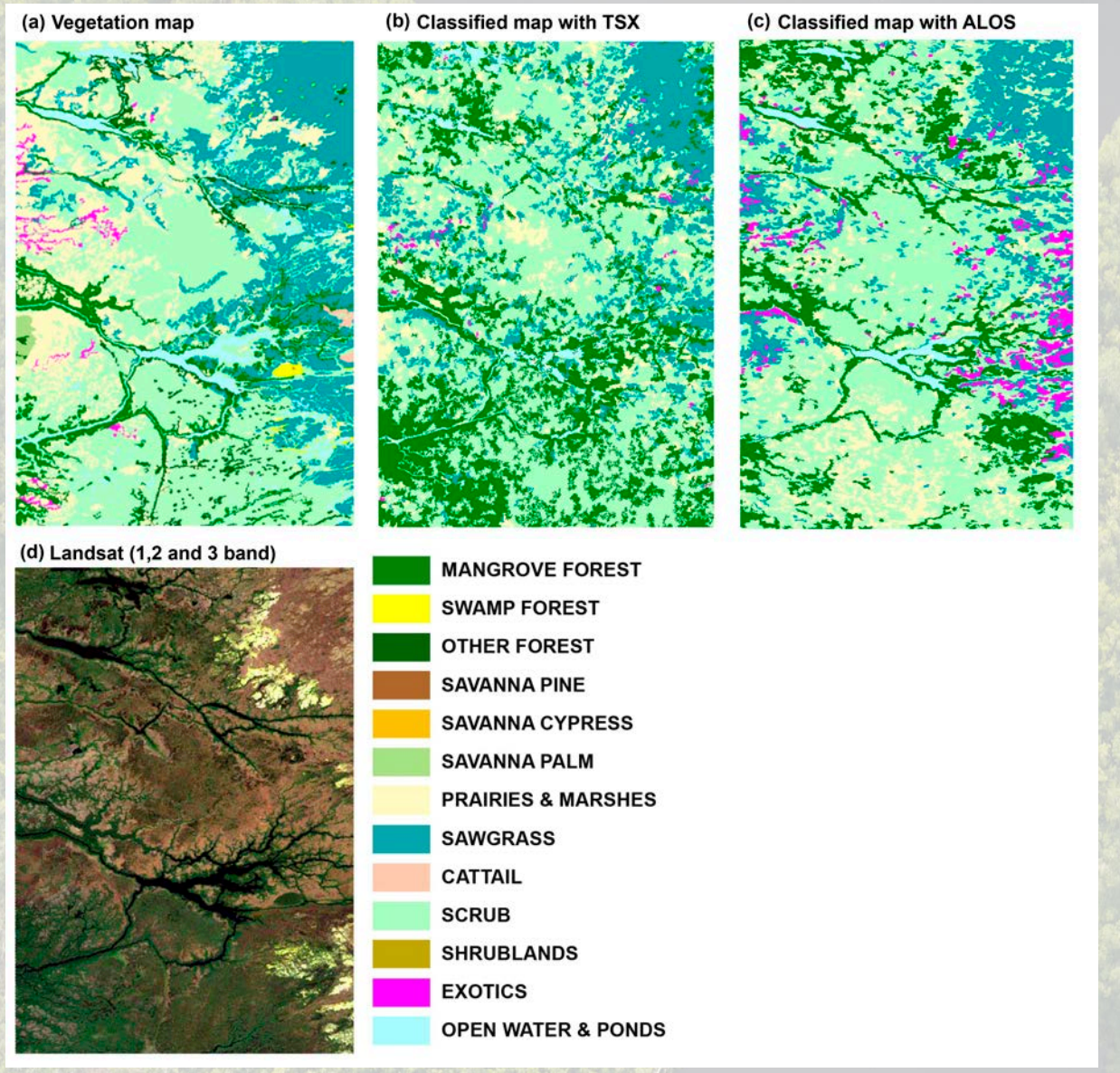

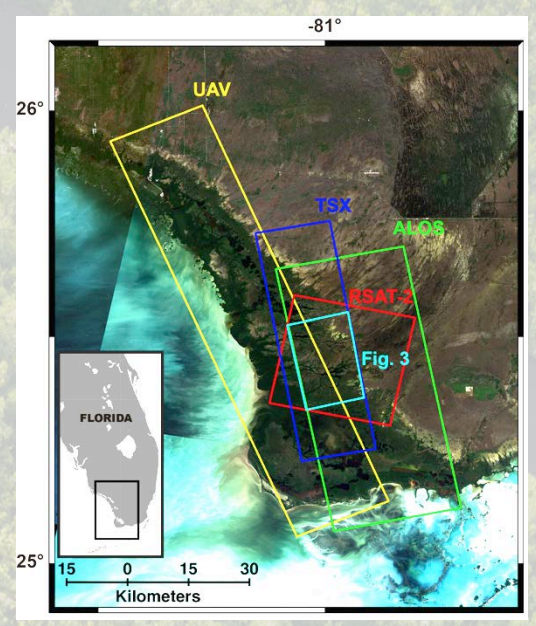

Limited success
52-57% fit to the vegetation map

However, the vegetation maps is old (data from the 1990's after Hurricane Andrew). Known to be unreliable.

Decompositions - UAVSAR

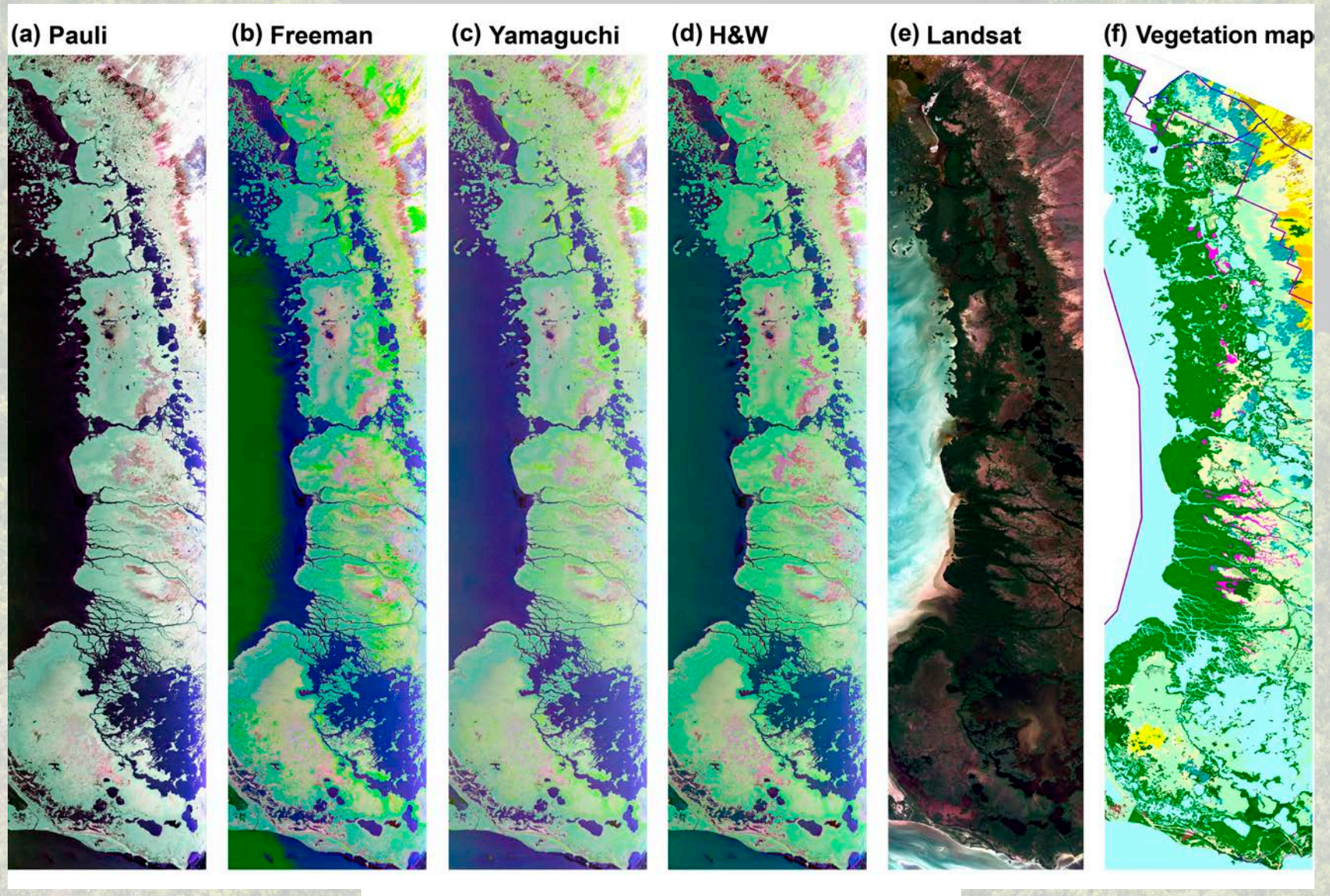

Characterization - comparison

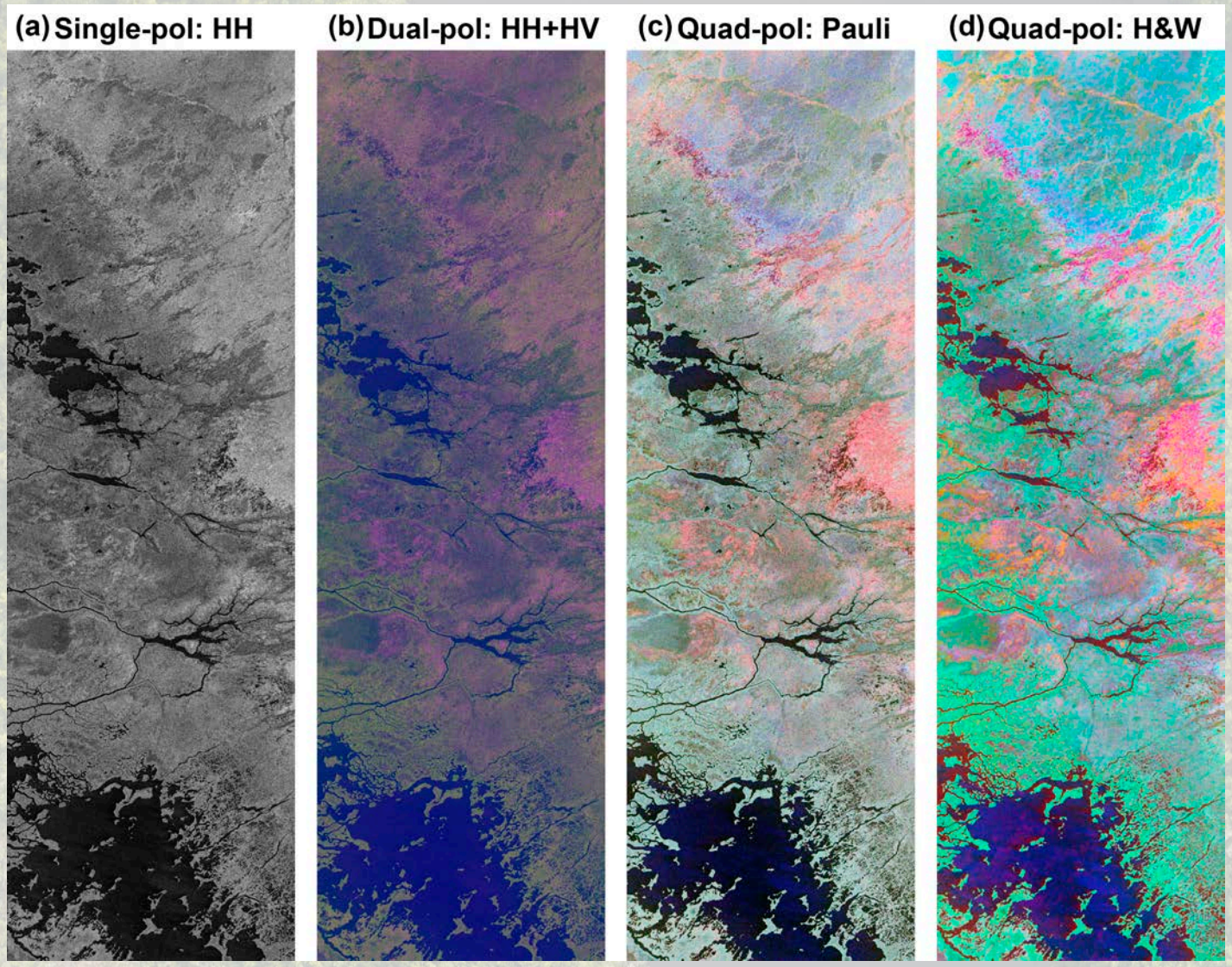

L-band
ALOS data

Increased sensitivity with increasing channels/components

Conclusions

- Pol-SAR decompositions are useful tool for characterizing tropical wetlands at all weather conditions.
- The 4-component decompositions (Yamaguchi, H-W) provide more detailed information than the 3-component ones (Pauli, Freeman).
- Decompositions based on C-band RSAT-2 data are less sensitive to vegetation variations compared to decompositions based on X-band (TSX) and L-band (ALOS) data.
- The Pol-SAR based vegetation map showed limited success (52-57% fit to the available map) and need further improvements.

Acknowledgements

- Data
  - DLR – TSX data
  - CSA (SOAR) – RSAT-2 data
  - JAXA & ASF – ALOS data

- Support
  - NASA
  - NSF
  - ESA